AIAA Journal
Vol. 37, No. 12, December 1999

Technical Notes

TECHNICAL NOTES are short manuscripts describing new developments or important results of a preliminary nature. These Notes cannot exceed 6 manuscript pages and 3 figures; a page of text may be substituted for a figure and vice versa. After informal review by the editors, they may be published within a few months of the date of receipt. Style requirements are the same as for regular contributions (see inside back cover).

Experiments in the Turbulent Near Wake of an Axisymmetric Body

A. I. Sirviente*
University of Michigan, Ann Arbor, Michigan 48109-2145
and
V. C. Patel†
University of Iowa, Iowa City, Iowa 52242-1580

I. Introduction

THE axisymmetric wake is an important member of canonical turbulent shear flows on which much of our current understanding of more general turbulent flows is based. Yet there are few reliable data, particularly in the near field, that can be used to elucidate how such a flow originates. Although many early measurements on axisymmetric wakes employed bluff bodies, data were obtained and analyzed only in the far field. The first experiment to report near-wake data, still excluding the separation region, was the well-known hot-wire measurements behind a prolate spheroid of axis ratio six of Chevray.[1] Calculations of Chen and Patel,[2] using Chevray's data as a test case, strongly suggested, though, that blockage effects may be significant in Chevray's data. Several other experiments on boundary layers on axisymmetric bodies have been reported since then, but only those of Patel and Lee[3] and Hyun[4] contain measurements in the wake. Hyun[4] and Hyun and Patel[5,6] performed experiments to study the near wake of an axisymmetric body with and without a propeller. Those without the propeller, made with a streamlined tail, are of interest here because the present measurements were made with the same body.

The experiments described here are part of a series[7–9] designed to study the evolution of axisymmetric wakes. Here we are concerned with the so-called drag wake of the body, in which the wake possesses a momentum deficit. Other experiments in this series are concerned with momentumless wakes, in which the body is propelled by a jet, without and with swirl. The propeller-flow experiments[4–6] conducted earlier also may be regarded as members of this series.

II. Experimental Arrangement

A new model of the axisymmetric body used by Hyun[4] (referred to in some earlier studies as the "Iowa Body") was constructed with the tail truncated at a diameter D of 3.96 cm to accommodate a jet of 3.90-cm diameter. For the present experiments the jet opening was closed. The modified body has a length L of 143.45 cm and a maximum radius R of 6.95 cm. The boundary layer on the body was tripped by a 1.2-mm-diam wire, located 9.5 cm from the nose. The experiments were conducted in the 1.07-m octagonal, open-test-section, return-circuit wind tunnel of the Iowa Institute of Hydraulic Research (Fig. 1). A cylindrical (x, r, θ) coordinate system, where x is measured from the base of the body, is used to report the data. In the steady axisymmetric flow considered here, the mean and fluctuating velocity components are denoted by (U, V, W) and (u, v, w), respectively.

The freestream velocity U_0 was set at 16.5 m/s, resulting in a Reynolds number based on body length $Re = U_0 L/\nu$ of 1.58×10^6, where ν is the kinematic viscosity of air. The model was mounted with a part of it extending into the tunnel contraction to enable measurements in the axial direction up to $x/L = 0.531$. (Although it may be preferable, for some purposes, to use the body base diameter D as a reference length, the body length L and radius R are chosen as reference lengths in the axial and radial direction, respectively, to facilitate comparison with the data of Hyun[4] and Hyun and Patel[5] and other experiments in this series.) In the radial direction, measurements were made up to $r/R = 4.5$ to recover the freestream conditions. Most of the measurements were made with a triple-sensor hot-wire probe and a five-hole pitot probe. The latter was used to determine the mean flow direction so that proper yaw and pitch angles for the hot-wire probe could be selected. It also provided redundant data for the mean-velocity components. The probes were traversed in the vertical direction by a simple computer-controlled mechanism. Measurements in the separated flow close to the base were made with a three-component fiber-optics laser Doppler velocimetry (LDV) system.[7] A manual traverse was used to move the LDV probe. Because this traverse was mounted 1.34 m from the tunnel centerline to meet the focal-length requirements of the probe, it did not interfere with the flow. A detailed description of the experimental equipment, instrumentation, tunnel characteristics, and measurement procedures can be found in Refs. 7 and 8, along with an analysis of the data uncertainty [2% for (U, V, W) and 10% for and $\overline{uu}$ and $\overline{uv}$].

III. Results

It is well known that the distance required for a free shear layer to attain self-similarity depends on the initial conditions. In the case of the wake of both a streamlined body[4] and a bluff body (present data), the initial conditions are set by the shape of the stern and the state of the boundary layer at the tail.

Measurements of the axial component of the mean velocity U and normal stress $\overline{uu}$ were made with radial traverses of a single hot wire at eight stations over the bluff body stern, three in the region $-0.180 < x/L < -0.115$, where the body is cylindrical, and the remainder where its surface has convex curvature. The boundary layer thickness δ increased rapidly from $0.12R$ at the first measurement station to about $0.63R$ at the tail. The present data are sufficient to define the boundary layer characteristics over the stern. At the first measurement station, $x/L = -0.180$, the boundary-layer integral parameters are

$$R_\theta = U_0\theta/\nu = 845$$

$$H = \frac{\delta_0^*}{\theta_0} = \int_0^\infty \left(1 - \frac{U}{U_0}\right) \mathrm{d}r \bigg/ \int_0^\infty \left(1 - \frac{U}{U_0}\right) \frac{U}{U_0}\, \mathrm{d}r = 1.29$$

$$C_f = \tau_w \big/ \left(\rho U_0^2/2\right) = 0.0045$$

[The wall shear stress τ_w and the friction velocity $u_\tau = \sqrt{(\tau_w/\rho)}$ were determined by use of a Clauser plot.] This station is located in the main test section of the wind tunnel, but the boundary layer is still recovering from the favorable pressure gradient of the tunnel contraction. This is evident from the low H and high C_f. These

---

Received 11 May 1998; revision received 26 July 1999; accepted for publication 29 August 1999.

*Assistant Professor, Department of Naval Architecture and Marine Engineering. Member AIAA.

†Professor and Director, Department of Mechanical Engineering, Iowa Institute of Hydraulic Research. Associate Fellow AIAA.

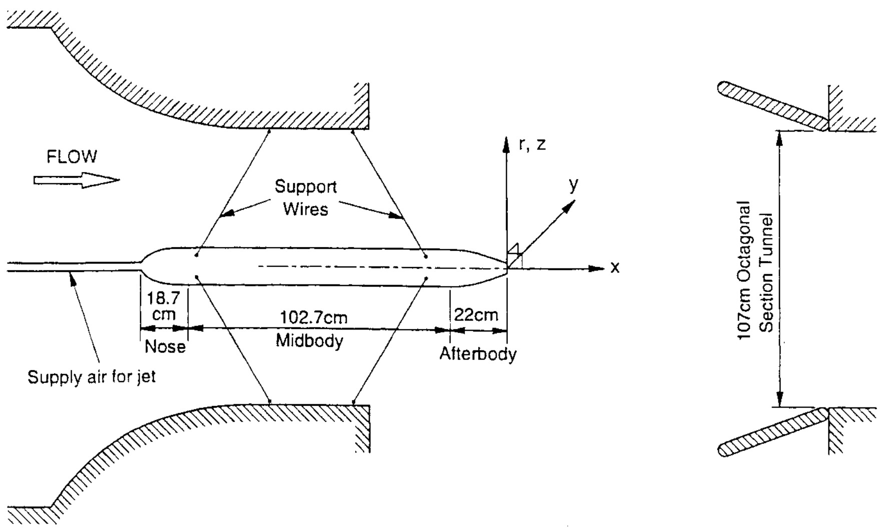

Fig. 1 Wind tunnel and model arrangement.

features should be noted when the data are used to test numerical methods and turbulence models. A very good agreement of friction velocity of the present data was found with the data of Hyun,[4] which suggests that truncation of the tail has a relatively minor effect on the stern boundary layer.

Extensive measurements were made, with different instruments, at 18 locations in the bluff body wake. The wake of the present body differs from that of the streamlined body[4] fitted with a dummy propeller hub, in the different extents of separated flow at the tail. For the bluff body, the region of reverse flow extended up to $x/R = 0.309$, compared with $x/R = 0.109$ behind the streamlined body. On the other hand, the radial extent of the reverse flow ($r/R = 0.285$), which is half the base diameter, is considerably larger than that on the streamlined body ($r/R = 0.05$). Measurements with the hot-wire and five-hole probes were discarded in and close to the region of reverse flow. These methods are unreliable in this region not only because they cannot resolve reverse flow but also because they are susceptible to larger errors in the presence of low mean velocities. Only the LDV data resolve the reverse flow. Well outside the reverse flow region, the LDV data are in agreement with those obtained by hot-wire and pressure probes. The latter is, of course, the only direct method for measuring the total and static pressures. For the present body, the drag coefficient C_D was found from the contribution of the mean velocity to the axial momentum at the last station: $C_D = 0.240$. This may be compared with $C_D = 0.113$ measured on the streamlined body.[4]

The total and static pressure distributions in the wake of the bluff body indicated that significant variation of static pressure occurred up to about $x/L = 0.2$ for the bluff body. The static pressure profile showed a region of high pressure in the center of the wake and continued variation of pressure outside the wake, $r > \delta$. This variation was consistent with the convex curvature of the mean streamlines as the boundary layer from the body enveloped the separation eddy, and the fact that the pressure decreased beyond δ indicated that the velocity at the edge of the wake, U_e, was less than the freestream velocity U_0. This meant that the velocity at the edge of the wake, U_e, normally used to define the velocity and length scales of wakes varied in the axial direction. By station $x/L = 0.063$, there no longer was reverse flow, but the effects of the convergence of the shear layer (the wall region of the upstream boundary layer) were expected to be large. At this station there was smaller variation of static pressure across the wake and a smaller, but still inward, radial component of velocity, indicating mean flow convergence toward the center line.

It is well known that the radius of an axisymmetric far (asymptotic, or self-similar) wake [defined as the radius b at which the local velocity defect $U_d = (U - U_c)$ is $U_d/2$, where U_c represents the centerline velocity] grows as $x^{1/3}$ while its velocity defect U_d decreases as $x^{-2/3}$. Both laws applied for the bluff body data at the last four stations, i.e., beyond about $x/L = 0.4$ (or 14.5 base diameters). Figure 2 shows the axial development of the centerline velocity defect and half-radius in the two wakes. The collapse of the data beyond about $x/L = 0.1$ is quite remarkable, particularly in view of the very different initial conditions and development close to the tail. The expected slower growth of the centerline velocity in the bluff body wake is clearly seen, however. This is associated with an initial decrease in the wake width until approximately $x/L = 0.15$, significantly close to the location where the static pressure becomes negligible. The latter suggested that the streamwise development of the bluff body wake may be viewed in three parts, the initial narrowing, the region where the similarity laws apply, and an intermediate region between the two. On the other hand, the streamlined body shows a continuous increase in the half-width parameter. Velocity profiles measured at comparable distances from the tails of both bodies in the range $x/L > 0.1$ were also contrasted.[7] Contrary to what might be expected in a wake starting from separated flow at the base, the mean velocity profiles of the present experiment showed a remarkably more rapid approach to similarity than the wake of the streamlined body. This rapid approach may be due to the fact that separation produces larger eddies closer in size to the large eddies responsible for mixing in the wake farther downstream.

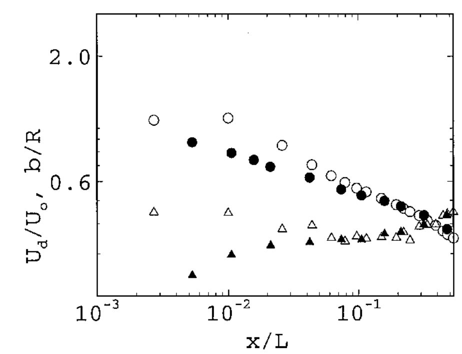

Fig. 2 Velocity (○, ●) and length scales (△, ▲) in wake of the bluff (○, △) and streamlined (●, ▲) body.

From similarity analysis, the maximum values of k $[(\overline{uu} + \overline{vv} + \overline{ww})/2]$, $\overline{uu}$, $\overline{uv}$, etc., should decay as $x^{-4/3}$, whereas the length scales associated with their profiles, such as the location of their maxima, should grow as $x^{1/3}$. The bluff body wake turbulence length scales approached the expected asymptotic behavior rather quickly, in about the same distance as b, but the intensities decayed much more slowly, as expected, and did not follow the mentioned power law even at the last stations. The turbulence kinetic energy (normalized by U_0) was found to be considerably smaller in the region of reverse flow of the bluff body compared with its value in the shear layer originating from the separating boundary layer of the

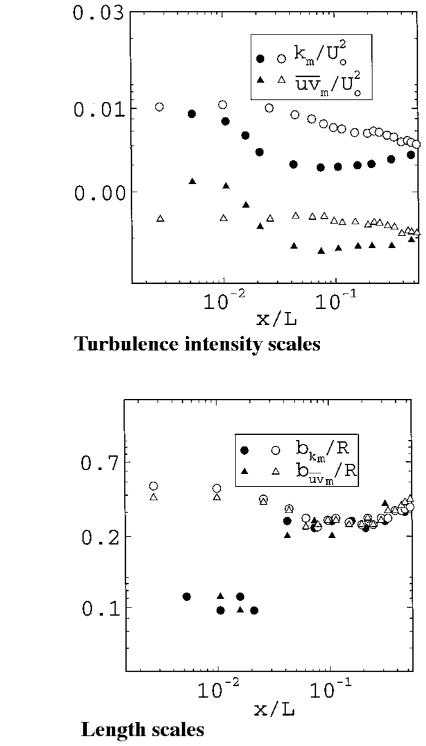

Fig. 3 Characteristic turbulence scales in wake of the bluff (○, △) and streamlined (●, ▲) body.

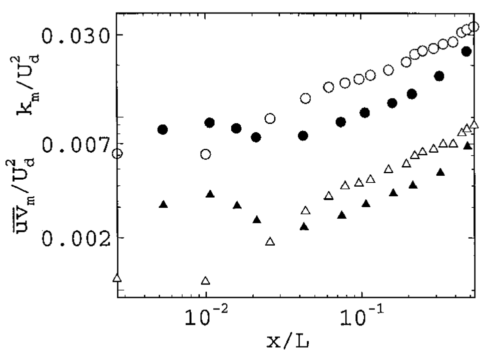

Fig. 4 Maximum turbulence kinetic energy (○, ●) and shear stress (△, ▲) in wake of the bluff (○, △) and streamlined (●, ▲) body.

body. However, it should be stressed that the local turbulence levels, referred to the local mean velocities, are large in the separation region, and this is one of the difficulties of measuring and modeling separated turbulent flow. In the near wake, there was a noticeable increase in the shear stress. This is most likely associated with the focusing of the wall turbulence in the upstream boundary layer as the shear layer converges to close the separation eddy. Further analysis of the data is needed to clarify this possibility.

The maxima of k and $\overline{uv}$ (designated as k_m and $\overline{uv}_m$) and their locations are compared in Fig. 3. Here the differences between the two sets of data due to separation are greater; k_m is much larger in the present case all along the wake, and $\overline{uv}_m$ is initially smaller and then larger. The locations of the maxima of the turbulence parameters clearly show the effect of separation. (Note the differences in $x/L < 0.1$.) However, despite the scatter, the streamwise evolution of the length scales suggests that they all follow the $\frac{1}{3}$ power law.

Yet another way to compare the evolution of the turbulence in the two wakes is to nondimensionalize the maximum values of the turbulence parameters by the local centerline velocity defect (Fig. 4). In this way the existence of equilibrium between mean and turbulent flow as well as between dissipation and production of turbulent energy is analyzed. Classical similarity analysis requires all of these ratios to approach constant values. It is clear that such absolute similarity is not reached in the experiments. In fact the data suggest a very slow trend, if any, toward such a condition. Similar results and trends have been documented in the wake of other streamlined bodies.[1,10] In Ref. 10, the equilibrium between mean and turbulent flow was not attained even after 40 diameters. On the other hand, the wakes behind bluff bodies such as a disk[11] or a sphere[12] exhibit a constant ratio between turbulent energy and total mean energy around 1.5 by four diameters. The ratio between maximum turbulent shear stress and centerline velocity defect is around 0.45–0.55 by 10 disk diameters. Bevilaqua and Lykoudis[11] compared the wake of a sphere with the wake of a porous disk having the same drag. They found that there were differences between both wakes in the structure of the turbulence and the scale of the mean flow, even after both had become self-preserving. In the present case, the wakes of the streamlined and bluff bodies attain a very similar state of development of both mean and turbulent flow fairly close to the body despite their large differences in drag coefficients.

IV. Conclusions

The measurements in the boundary layer and wake of the bluff axisymmetric body reported here complement previous studies of axisymmetric wakes insofar as they provide detailed information on the streamwise development of the wake from a separated boundary layer at the tail to its self-similar state. The characteristics of the thick stern boundary layer were found to be similar to those in measurements[4] of the corresponding streamlined bodies. Truncation of the tail, resulting in a bluff body, did not significantly alter the boundary-layer development up to that point. The (mean) separation bubble in the wake extends to approximately $x/L = 0.015$, or $x/D_b = 0.542$, where D_b is the base diameter. Significant variations of pressure in the radial and axial directions are found until about $x/L = 0.2$ ($x/D_b = 7.25$). This region is termed the "near wake." The intermediate region of the wake extends approximately over the axial distance $0.2 < x/L < 0.4$ ($7.25 < x/D_b < 14.5$). In this region, the flows from the near-wall and outer regions of the stern boundary layer interact and mix up to the center of the wake, producing a fully mixed wake downstream. The half-radius and centerline velocity defect of the wake follow power laws derived from similarity analysis beyond about $x/L = 0.4$ ($x/D_b = 14.5$). The velocity profiles become self-similar, but the turbulence profiles do not. Comparisons of the present data with those in the wake of the same body with a streamlined tail[4] revealed that the principal parameters of the two wakes collapse beyond about $x/L = 0.1$ despite the very different initial conditions and differences in the drag coefficient.

References

[1]Chevray, R., "The Turbulent Wake of a Body of Revolution," *Journal of Basic Engineering*, Vol. 90, June 1968, pp. 275–284.

[2]Chen, H. C., and Patel, V. C., "Evolution of Axisymmetric Wakes from Attached and Separated Flows," *Turbulent Shear Flow VI*, Springer–Verlag, New York, 1988, pp. 215–231.

[3]Patel, V. C., and Lee, Y. T., "Thick Axisymmetric Turbulent Boundary Layer and Near Wake of a Low-Drag Body of Revolution," Iowa Inst. of Hydraulic Research, IIHR Rept. 210, Univ. of Iowa, Iowa City, IA, 1977.

[4]Hyun, B. S., "Measurements in the Flow Around a Marine Propeller at the Stern of an Axisymmetric Body," Ph.D. Dissertation, Mechanical Engineering Dept., Univ. of Iowa, Iowa City, IA, 1990.

[5]Hyun, B. S., and Patel, V. C., "Measurements in the Flow Around a Marine Propeller at the Stern of an Axisymmetric Body. Part I. Circumferentially-Averaged Flow," *Experiments in Fluids*, Vol. 11, April 1991, pp. 33–44.

[6]Hyun, B. S., and Patel, V. C., "Measurements in the Flow Around a Marine Propeller at the Stern of an Axisymmetric Body. Part II. Phase-Averaged Flow," *Experiments in Fluids*, Vol. 11, May 1991, pp. 105–117.

[7]Sirviente, A. I., "Wake of an Axisymmetric Body Propelled by a Jet with and Without Swirl," Ph.D. Dissertation, Mechanical Engineering Dept., Univ. of Iowa, Iowa City, IA, 1996.

[8]Sirviente, A. I., and Patel, V. C., "Wake of a Self-Propelled Body, Part 1: Momentumless Wake," *AIAA Journal* (to be published).

[9]Sirviente, A. I., and Patel, V. C., "Wake of a Self-Propelled Body, Part 2: Momentumless Wake with Swirl," *AIAA Journal* (to be published).

[10]Schetz, J. A., and Jakubowski, A. K., "Experimental Studies of the Turbulent Wake Behind Self-Propelled Slender Bodies," *AIAA Journal*, Vol. 13, No. 10, 1975, pp. 1568–1575.

[11]Bevilaqua, P. M., and Lykoudis, P. S., "Turbulence Memory in Self-Preserving Wakes," *Journal of Fluid Mechanics*, Vol. 89, July 1978, pp. 589–606.

[12]Carmody, T., "Establishment of the Wake Behind a Disk," *Journal of Basic Engineering*, Vol. 87, Dec. 1964, pp. 869–882.

F. W. Chambers
Associate Editor

Hemisphere-Cylinder in Dynamic Pitch-Up Motions

O. K. Rediniotis*
Texas A&M University, College Station, Texas 77843-3141
N. T. Hoang†
AURORA Flight Sciences Corporation, Manassas, Virginia 20110
and
D. P. Telionis‡
Virginia Polytechnic Institute and State University, Blacksburg, Virginia 24061

I. Introduction

THE flows over various axisymmetric bodies such as ogive-cylinders, hemisphere-cylinders, and prolate spheroids have been studied numerically and experimentally by many investigators. An extensive literature review can be found in Ref. 1. An interesting feature of the flow over axisymmetric bodies at large incidence is the asymmetry of the mean vortical patterns of the wake. This phenomenon has been well documented for pointed bodies such as conical and ogive-cylinder bodies.[2,3] Flows over such bodies are sensitive to many parameters, such as irregularities at the nose, surface roughness, body length, slenderness of the nose, angle of attack, freestream turbulence, and Reynolds number. Moskovitz et al.[2] investigated the effects of geometric perturbations on the asymmetric flow past an ogive/cone cylinder. Roos and Kegelman[3] studied asymmetric flows at angles of attack up to 60 deg over three generic forebodies, namely ogive, elliptical, and chined bodies. Blunt-nosed models are less prone to asymmetry. Forced asymmetric wake patterns over blunt-nosed cylinders have been experimentally documented by Hoang and Telionis.[4]

In all of these efforts, steady-state flowfields with the models at fixed angles of attack were investigated. Very little has been published on the flowfield development over dynamically maneuvering bodies. A numerical investigation was carried out by Ying et al.[5] on dynamic motions of slender bodies. However, the work was not substantiated by experimental comparison. Stanek and Visbal[6] have also calculated the flow over a pitching slender body. The reduced pitch rates employed there were much larger than the ones considered here. Experimental efforts on pitching slender bodies have been confined to flow visualizations or force measurements.[7–9]

The purpose of the present investigation is to extend our understanding of the development of the leeward vortices over a hemisphere-cylinder and, in particular, asymmetric leeward vortices under unsteady conditions. This was accomplished by placing a hemisphere-cylinder model in a steady flowfield and mechanically pitching it about its nose. The unsteady development of the wake is studied. To induce vortex asymmetry a disturbance is introduced on the nose of the hemisphere-cylinder.

Received 16 June 1997; revision received 20 March 1998; accepted for publication 8 March 1999.

*Assistant Professor, Aerospace Engineering Department.
†Research Scientist.
‡Frank J. Maher Professor, Engineering Mechanics Department.

II. Facilities, Instrumentation, and Experimental Conditions

The work was conducted in the Engineering Science and Mechanics (ESM) water tunnel through laser Doppler velocimetry (LDV). The water tunnel has a 25.4 × 30.5 cm test section and can achieve speeds up to 3 m/s at turbulence levels ranging from 0.6 to 1.5%. Three-component LDV was employed in the water tunnel. The system employed is a Thermal Systems, Inc. (TSI) LDV system operating in backscatter mode with a 35 mW helium–neon laser. An assembly of mirrors and traversing mechanisms operated by stepping motors facilitates displacement of the measuring volume. Measuring grids normal to the oncoming stream can thus be automatically traversed. The measuring volume can be positioned on a grid point with an accuracy of 0.1 mm through the use of two linear variable differential transformers (LVDTs) that are integrated in a position feedback loop. The entire data-acquisition operation is controlled by serially communicating laboratory computers that are programmed to operate the pitching mechanism and the traversing systems, collect the information on the instantaneous angle of attack, perform the LDV data acquisition, reduce the data, and transfer the data to a mainframe IBM 3090 for postprocessing and presentation. Detailed information on the LDV instrumentation and data-acquisition scheme can be found in Ref. 10. The hemisphere-cylinder model tested was provided by the Fluid Dynamics Branch of NASA Langley Research Center. The model was machined out of aluminum, with an overall length of $L = 14.73$ cm and a diameter of $D = 2.95$ cm.

Experiments were conducted with a fixed as well as with a dynamically pitching model. The dynamic motion chosen was a pitch-up about the nose, followed by a slow return to the initial angle of attack. Data were obtained at 100 time instants during the pitch-up and were ensemble averaged. To decide on the number of realizations per ensemble average, we took measurements over 50 realizations at representative wake locations. For each location, ensemble averages

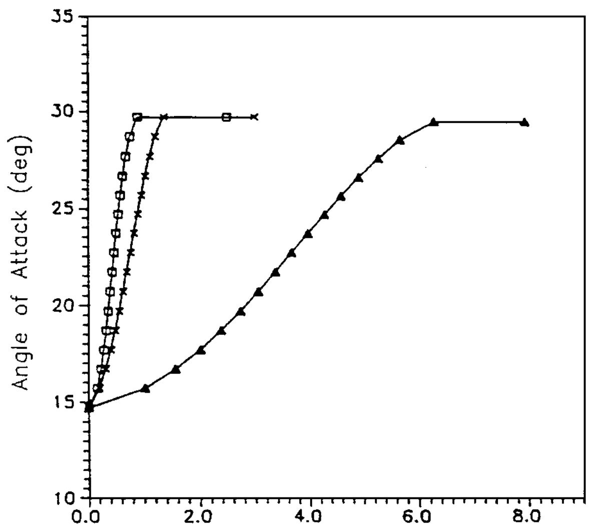

Fig. 1 Time schedules for the pitch-up motions: ▲, $k_2 = 1.4 \times 10^{-3}$; ×, $k_3 = 6 \times 10^{-3}$; and □, $k_4 = 1 \times 10^{-2}$.

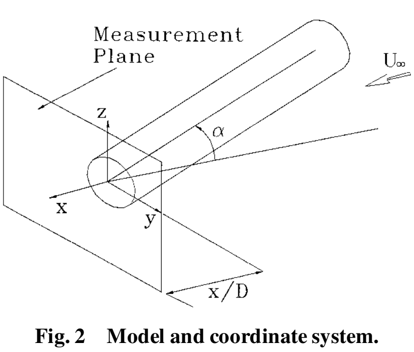

Fig. 2 Model and coordinate system.